Different dynamic accumulation and toxicity of ZnO nanoparticles and ionic Zn in the soil sentinel organism Enchytraeus crypticus

He, Erkai; Qiu, Hao; Huang, Xueyin; Van Gestel, Cornelis A.M.; Qiu, Rongliang

published in
Environmental Pollution
2019

DOI (link to publisher)
10.1016/j.envpol.2018.11.037

document version
Publisher's PDF, also known as Version of record

citation for published version (APA)
He, E., Qiu, H., Huang, X., Van Gestel, C. A. M., & Qiu, R. (2019). Different dynamic accumulation and toxicity of ZnO nanoparticles and ionic Zn in the soil sentinel organism Enchytraeus crypticus. *Environmental Pollution*, *245*, 510-518. https://doi.org/10.1016/j.envpol.2018.11.037

Environmental Pollution 245 (2019) 510–518

Contents lists available at ScienceDirect

Environmental Pollution

journal homepage: www.elsevier.com/locate/envpol

Different dynamic accumulation and toxicity of ZnO nanoparticles and ionic Zn in the soil sentinel organism *Enchytraeus crypticus*☆

Erkai He [a], Hao Qiu [b, c, *], Xueyin Huang [a], Cornelis A.M. Van Gestel [d], Rongliang Qiu [a, e]

[a] School of Environmental Science and Engineering, Sun Yat-sen University, Guangzhou, 510275, China
[b] School of Environmental Science and Engineering, Shanghai Jiao Tong University, Shanghai, 200240, China
[c] Shanghai Institute of Pollution Control and Ecological Security, Shanghai, 200092, China
[d] Department of Ecological Science, Faculty of Science, Vrije Universiteit, De Boelelaan 1085, 1081HV, Amsterdam, the Netherlands
[e] Guangdong Provincial Key Laboratory of Environmental Pollution Control and Remediation Technology, Guangzhou, 510275, China

ARTICLE INFO

Article history:
Received 19 July 2018
Received in revised form
9 November 2018
Accepted 12 November 2018
Available online 15 November 2018

Keywords:
Toxicity
Uptake
ZnO nanoparticles
Toxicokinetics
Toxicodynamics

ABSTRACT

There is still no consensus over the specific effects of metal-based nanoparticles when compared with the conventional metal salts. Here, the accumulation and toxicity of ZnO-NPs and $ZnCl_2$ in *Enchytraeus crypticus* over time (1–14 d) were investigated using a sand-solution exposure medium and applying a toxicokinetics and toxicodynamics approach. For both Zn forms, body Zn concentration in the organisms was dependent on both the exposure concentration and exposure time, with equilibrium being reached after 7–14 days of exposure. Generally, the uptake and elimination rate constants (K_u and K_{e1}) were smaller for ZnO-NPs (5.74–12.6 mg $kg^{-1}d^{-1}$ and 0.17–0.39 d^{-1}) than for $ZnCl_2$ (8.32–40.1 mg $kg^{-1}d^{-1}$ and 0.31–2.05 d^{-1}), suggesting that ionic Zn was more accessible for *E. crypticus* than nanoparticulate Zn. Based on external exposure concentrations, LC50s for ZnO-NPs and $ZnCl_2$ decreased with time from 123 to 67 Zn mg L^{-1} and from 86 to 62 Zn mg L^{-1}, reaching an almost similar ultimate value within 14 d. LC50s based on body Zn concentrations were almost constant over time (except for 1 d) for both ZnO-NPs and $ZnCl_2$, with overall $LC50_{body}$ of Zn being 1720 and 1306 mg kg^{-1} dry body weight, respectively. Body Zn concentration, which considers all available pathways, was a good predictor of dynamic toxicity of $ZnCl_2$, but not for ZnO-NPs. This may be attributed to the specific internal distribution and detoxification mechanisms of ZnO-NPs. The particles from ZnO-NPs dominated the accumulation (>75%) and toxicity (~100%). Our results suggest that dynamic aspects should be taken into account when assessing and comparing NPs and metals uptake and consequent patterns of toxicity.

1. Introduction

Metal-based nanoparticles (NPs) have been extensively applied in modern technology due to their unique physiochemical properties, e.g., small size, high surface area and high surface reactivity (Ma et al., 2013). One of the most widely used metal oxide nanoparticles are ZnO-NPs (Bandyopadhyay et al., 2015). These NPs may eventually enter the soil environment in high amounts during all stages of their life cycle, including production, recycling and disposal. Hence, there is an increasing concern about the potential adverse effects of ZnO-NPs on environmental receptors (Khan et al., 2015). A thorough evaluation of the impact of ZnO-NPs on terrestrial organisms is therefore needed for the purpose of risk assessment and regulation.

ZnO-NPs may exert toxic effects on, for instance, water fleas (*Daphnia magna*), zebrafish embryos (*Danio rerio*), and springtails (*Folsomia candida*) (Adam et al., 2015; Hua et al., 2014; Kool et al., 2011), but there is still no consistent conclusion as to what extent the metal-based nanoparticles are more toxic than the corresponding free Zn ions. For instance, the aquatic toxicity of different zinc forms to *D. magna* followed the order: ZnO-NPs > $ZnSO_4$ > bulk ZnO (Heinlaan et al., 2008), whereas Franklin et al. (2007) found similar toxicity of ZnO-NPs, bulk ZnO and $ZnCl_2$ to a freshwater alga. In case of metal-based nanoparticles, both the nanoscale size of the particles and the release of metal ions may contribute to uptake and effects (Li et al., 2015; Tourinho et al., 2012). Miao et al. (2010) found that ZnO-NP toxicity to marine diatoms could be

☆ This paper has been recommended for acceptance by Bernd Nowack.

* Corresponding author. School of Environmental Science and Engineering, Shanghai Jiao Tong University, Shanghai, 200240, China.
E-mail address: haoqiu@sjtu.edu.cn (H. Qiu).

https://doi.org/10.1016/j.envpol.2018.11.037
0269-7491/

solely explained by Zn^{2+} release. In contrast, when studying the toxicity of Cu-NPs and ZnO-NPs to *D. magna*, Xiao et al. (2016) found that particles rather than the dissolved ions were the major source of toxicity. Li et al. (2015) reported that both particulate silver and released Ag ions contributed to the toxicity of Ag-NPs to earthworms cultured in solution. Major uncertainties are with assessing exposure and the role of the particles and free ions released. One way of tackling this problem is by looking at the uptake of nanoparticles and released ions and relating toxicity not only to external exposure concentrations but also to body burdens (Ribeiro et al., 2015; Tourinho et al., 2016). The notion that toxic effects will only occur when chemicals are able to enter the cells of an organism probably will also hold for nanoparticles, although it will be a challenge to trace the exact pathways and forms of uptake in organisms (Schultz et al., 2015).

Another important factor to consider when assessing the risk of nanoparticles is time. Both fate of nanoparticles in the environmental and their uptake and effects in organisms are prone to change with time (Diez-Ortiz et al., 2015; Waalewijn-Kool et al., 2013). As a consequence, a dynamic approach is warranted. Toxicokinetic and toxicodynamic models have been successfully used to describe the dynamic uptake, elimination and induction of toxic effects for conventional metals in organisms (He and van Gestel, 2013; Jager et al., 2011). However, comparative study on the uptake and effects of metal-based nanoparticles and their counterparts from the perspective of toxicokinetic and toxicodynamic processes is still limited. Insights into these dynamic processes could help to elucidate the possible (subtle) differences between different metal forms.

Against this background, this study aimed to evaluate the dynamic uptake and toxicity of ZnO-NPs in comparison to $ZnCl_2$ for an ecologically important soil species *Enchytraeus crypticus*. Special emphasis was put on 1) identifying the differences between the two forms of Zn from the angle of toxicokinetics and toxicodynamics; 2) determining whether the body Zn concentration represented a better dose descriptor for predicting the effects of ZnO-NPs and $ZnCl_2$; 3) determining the relative contribution of nanoparticulate Zn and ionic Zn to the overall accumulation and toxicity.

2. Materials and methods

2.1. Chemicals and characterization

ZnO-NPs (Sigma-Aldrich, nominal size <50 nm) and $ZnCl_2$ (Sigma-Aldrich, >99%) were selected as the target toxicants. The morphology and size of the ZnO-NPs were characterized by scanning electron microscopy (SEM, JSM-6330F, JEOL Ltd, Japan). The size distribution and zeta potential of ZnO-NP suspensions of 10, 40 and 160 Zn mg L^{-1} after 0 h–168 h incubation were determined with dynamic light scattering (DLS, Omni, Brookhaven, America).

2.2. Test organism

Enchytraeus crypticus (class Oligochaeta, family Enchytraeidae) were selected as the test organism because they are widespread in various soil types and sensitive to both inorganic and organic chemicals (Castro-Ferreira et al., 2012). *E. crypticus* were cultured in a climate chamber at 20 °C, relative humidity of 75%, and complete darkness. They were regularly fed with oat meal and yolk powder. Adults with white spots in the clitellum region were used for the toxicity and bioaccumulation tests.

2.3. Exposure medium

Basic solution (composed of 0.2 mM Ca^{2+}, 0.05 mM Mg^{2+}, 2.0 mM Na^{+} and 0.078 mM K^{+}) was prepared to simulate the composition of soil solution. The ZnO nanoparticles were added to the basic solution to obtain a stock suspension, which was shaken and sonicated for 15 min in a water bath sonicator. The ZnO-NP stock suspension was further diluted to prepare the test suspensions. The pH of the test suspensions was adjusted to 6.5 (±0.1) with MOPS (3-[N-morpholino] propane sulfonic acid) and MES (2-[N-morpholino] ethane sulfonic acid) buffers. Similar procedures were followed to obtain $ZnCl_2$ solutions of different concentrations.

A sand-solution system was used as the test medium in the present study. Quartz sand was combusted at 600 °C and washed with 0.1 M HNO_3 to get rid of organic and inorganic matter (He and van Gestel, 2013). For each replicate, 5.5 mL of test suspension/solution was added to 20 g quartz sand and equilibrated for one day before starting the toxicity and bioaccumulation tests.

2.4. Toxicity and accumulation tests

The dynamic toxicity and uptake tests with ZnO-NPs and $ZnCl_2$ were performed with five sets of exposure times: 1, 4, 7, 10 and 14 days. Each set contained a concentration gradient of ZnO-NPs (0, 10, 20, 30, 40, 60, 90, 120, 150, 180, 240 Zn mg L^{-1}) and $ZnCl_2$ (10, 20, 30, 40, 60, 90 and 120 Zn mg L^{-1}). For each treatment, 10 adult test organisms were exposed to the sand-solution system, and three replicates were used for each exposure concentration and time. The test was conducted in the climate chamber at 20 °C, 75% relative humidity, and 16 h light/8 h dark. At the end of the test, mortality of the test organisms was determined. Depending on the number of surviving animals, for each replicate 2 to 5 individuals were collected and washed with deionized water to remove the surface-bound Zn. The collected animals were frozen at −18 °C for further analysis.

2.5. Metal analysis

The ZnO-NP suspensions and freeze-dried animals were digested with concentrated HNO_3. The actual total concentrations of Zn in the ZnO-NP suspensions, $ZnCl_2$ solution, and test animals were measured with inductively coupled plasma optical emission spectrometry (ICP-OES, Optima 5300DV, PE), with the detect limit of the ICP-OES analysis being 0.001 mg L^{-1}. The certified reference material DOLT-4 (Dogfish liver) was used as quality control, and measured Zn concentrations never differed more that 10% from the certified value, showing the good recovery of Zn. The mean value of the measured Zn body concentrations and survival fraction of three replicates was used for data analysis and model fitting.

2.6. Dynamic accumulation and toxicity modeling

The accumulation of Zn in the test organisms with time was described with a one-compartment model, which considers the balance between assimilation and excretion.

$$C_{body}(t) = C_0 \times e^{-K_{e1} \times t} + \frac{K_u \times C_w}{K_{e1}} \times (1 - e^{-K_{e1} \times t}) \quad (1)$$

where $C_{body}(t)$ is the body Zn concentration after different exposure times (mg kg^{-1}), t the exposure time (d), C_0 is the initial or background body Zn concentration (mg kg^{-1}); C_w the exposure concentration (mg L^{-1}), K_u the uptake rate constant (mg $kg^{-1}d^{-1}$), and K_{e1} the bioaccumulation-based elimination rate constant (d^{-1}).

The relationship between the fraction of surviving animals (S) and Zn exposure concentration was described with a logistic dose-response model.

$$S = \frac{S_{max}}{1 + (\frac{x}{x_{50}})^b} \quad (2)$$

where S_{max} is survival fraction of control (%), x the dose descriptor (i.e., total Zn concentration in the test solution ([Zn], mg L^{-1}) and in the animals ($[Zn]_{body}$, mg kg^{-1}), x_{50} the corresponding effective concentration that causes 50% mortality (i.e., LC50 and $LC50_{body}$), and b the slope parameter.

The relationship between toxicity and exposure time was explained in terms of Zn elimination kinetics.

$$LC50\ (t) = \frac{LC50\infty}{1 - e^{-K_{e2} \times t}} \quad (3)$$

where LC50(t) is the LC50 value after different exposure times (mg L^{-1}), LC50∞ the ultimate LC50 value (mg L^{-1}), and K_{e2} toxicity-based elimination rate constant (d^{-1}). The parameters were estimated by the nonlinear regression analysis using Origin 2016 (OriginLab, USA).

2.7. Determining the relative contribution of nanoparticulate and ionic Zn

To investigate the dynamic release of Zn^{2+} from ZnO-NPs, ZnO-NP suspensions with initial concentrations of 10, 40 and 160 Zn mg L^{-1} were prepared with basic solution. For each concentration, five sampling time points (1 h, 24 h, 48 h, 96 h, 168 h, 240 h and 336 h) were selected. The amount of released Zn ions was determined by ultrafiltration of the suspensions over a 30 *K*Da ultrafilter (Sartorius) and centrifugation for 25 min at 4000 rpm, 20 °C, until most of the solution had passed the filter. In this way, the particulate ZnO ($ZnO\text{-}NP_{(particle)}$) could be retained on the filter, while the released Zn^{2+} ($ZnO\text{-}NP_{(ion)}$) could be determined by measuring the Zn concentration in the ultrafiltrate.

The response addition (RA) model is often used for predicting the effects of mixtures of toxicants that are believed to have dissimilar modes of action (Qiu et al., 2016). Several studies have suggested that metal ions and metal-based nanoparticles possess dissimilar modes of action (Hua et al., 2014; Xiao et al., 2015). Hence, in the present study, the RA model was chosen for calculating the relative contribution of $NP_{(particle)}$ and $NP_{(ion)}$ to the toxicity of ZnO-NP suspensions.

$$E_{(total)} = 1 - [(1 - E_{(ion)}) \times (1 - E_{(particle)})] \quad (4)$$

where $E_{(total)}$ and $E_{(ion)}$ represent the toxicity caused by the suspension and the corresponding released ions. In the present study, $E_{(total)}$ and $E_{(ion)}$ were experimentally determined. This makes $E_{(particle)}$ the only unknown, allowing for direct calculation of the effects caused by the $NP_{(particle)}$.

By incorporating the estimated K_u and K_e of $ZnCl_2$ into Eq. (1), the contribution of $ZnO\text{-}NP_{(ion)}$ to the bioaccumulation of Zn after different exposure times was calculated, using the concentrations of released Zn ions in ZnO-NP suspensions as inputs. Because the total body concentration was measured experimentally, the contribution of $ZnO\text{-}NP_{(particle)}$ to Zn bioaccumulation could be derived. The definitions of all parameters in Eq. (1) to Eq. (4) are shown in Table S1.

3. Results

3.1. Physicochemical properties and ion release of ZnO-NPs

The SEM analysis demonstrated that the ZnO-NPs used in this study mainly existed as spherical particles with diameters between 24 and 48 nm (Fig. 1). The size distributions of the ZnO-NPs after 0, 1, 5, 24, 96 and 168 h of suspension are shown in Table S2. The NPs aggregated as soon as they were spiked into the test solutions. Generally, particle size of the ZnO-NPs in the suspensions increased with increasing total concentration and incubation time. From 0 to 168 h, mean (±SD, n = 5) particle size increased from 385 (±20.5) nm at 0 h to 1500 (±275) nm at 168 h for 9.99 Zn mg L^{-1} of ZnO-NPs, from 258 (±11.7) to 1450 (±98.4) nm for 40.6 Zn mg L^{-1} of ZnO-NPs, and from 497 (±12.9) to 1539 (±83.2) nm for 174 Zn mg L^{-1} of ZnO-NPs. The initial zeta potential was 28.6, 33.2, and 29.1 mV, respectively, for ZnO-NPs in solutions at concentrations of 9.99, 40.6 and 174 Zn mg L^{-1}.

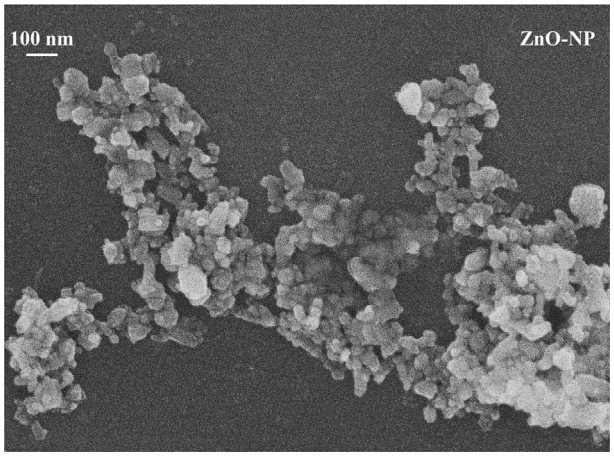

Fig. 1. TEM images of the ZnO-NPs tested in this study under a scale range of 100 nm.

The ion release profiles of the ZnO-NPs from 1 h to 336 h (14d) are shown in Fig. 2. The ZnO-NPs gradually dissolved with increasing incubation time, with the percentage of released Zn ions in ZnO-NP suspensions of 9.99, 40.6, and 174 Zn mg L^{-1} increasing from 19.3% to 31.5%, from 7.14% to 14.8%, and from 1.38% to 2.40%, respectively. The higher ZnO-NP concentrations therefore resulted in a lower ion release rate. However, the total amounts of released ions at each time point were similar, e.g., the concentrations of released Zn ions after 336 h were 3.15, 4.35, and 4.17 mg L^{-1} for the

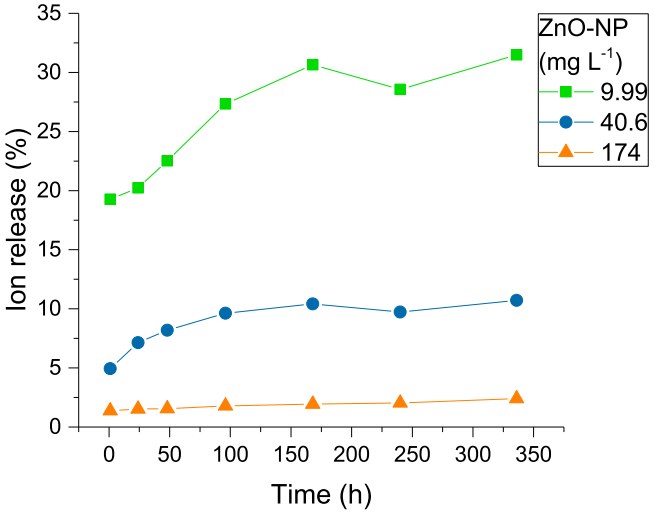

Fig. 2. Relative dissolved Zn ion release (in% of total Zn concentration) from ZnO-NP suspensions at concentrations of 9.99, 40.6 and 174 Zn mg L^{-1} after different incubation times.

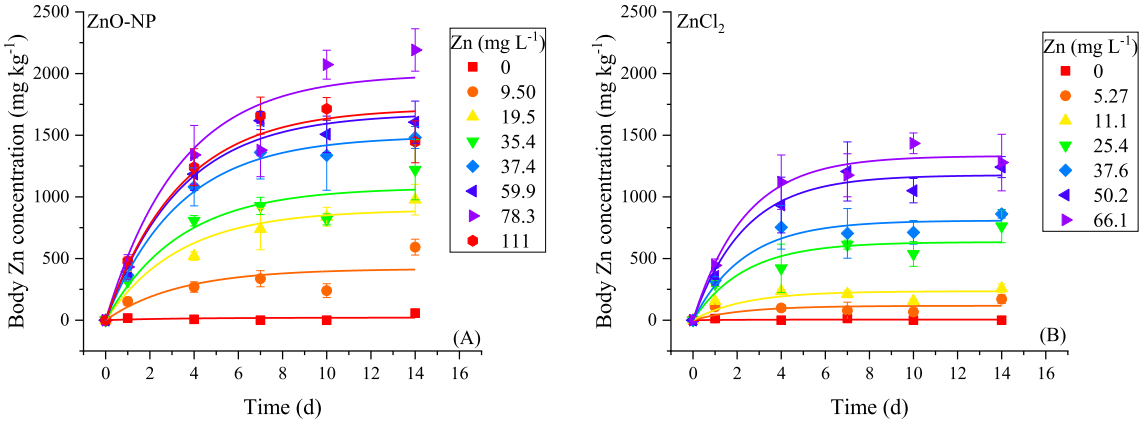

Fig. 3. Relationship between body Zn concentration (Zn mg kg^{-1} dry body weight) and exposure time in *Enchytraeus crypticus* exposed to different concentrations of ZnO-NPs and $ZnCl_2$ in test solutions embedded in a quartz sand matrix. Data points show the mean values of observed data with standard error, solid lines show the fit of the one-compartment model (Eq. (1)) to the body metal concentration data at different Zn exposure levels separately.

9.99, 40.6, and 174 Zn mg L^{-1} ZnO-NPs treatments, respectively.

3.2. Dynamic accumulation of ZnO-NPs and $ZnCl_2$ in E. crypticus

For both the ZnO-NP and $ZnCl_2$ treatments, body Zn concentrations in *E. crypticus* increased with increasing exposure level and exposure time (Fig. 3). After 10–14 days of exposure, the body Zn concentrations reached steady state. The maximum body Zn concentrations were 2191 (±172) mg kg^{-1} for the ZnO-NP series and 1434 (±83.8) mg kg^{-1} for the $ZnCl_2$ series. At similar Zn exposure levels, body Zn concentration was higher for ZnO-NPs than for $ZnCl_2$ treatments, e.g. for ZnO-NP (37.4 Zn mg L^{-1}) and $ZnCl_2$ (37.6 Zn mg L^{-1}) treatments, after 14 d exposure body Zn concentrations reached 1220 (±244) mg kg^{-1} and 861 (±33.9) mg kg^{-1}, respectively.

When fitting data for each exposure concentration separately using Eq. (1), with increasing Zn exposure levels, for ZnO-NPs the uptake rate constant K_u peaked at 12.6 mg $kg^{-1}d^{-1}$ at 37.4 Zn mg L^{-1} and significantly decreased to 5.74 mg $kg^{-1}d^{-1}$ at 111 Zn mg L^{-1} ($p < 0.01$). For $ZnCl_2$, K_u decreased from 40.1 to 8.32 mg $kg^{-1}d^{-1}$ with exposure concentrations increasing from 5.27 to 25.4 Zn mg L^{-1}, and then leveled off ($p = 0.06$) (Table 1). The estimated bioaccumulation-based elimination rate constant K_{e1} values for ZnO-NPs (0.17–0.39 d^{-1}) and $ZnCl_2$ (0.31–0.42 d^{-1}) remained almost constant across the different Zn exposure levels, except for the two lowest exposure concentrations of $ZnCl_2$. Generally, compared with ZnO-NPs, $ZnCl_2$ exposure resulted in a higher Zn uptake and elimination rate constants in *E. crypticus*. The body Zn concentrations estimated using the one-compartment model (Eq. (1)) with K_u and K_{e1} are shown in Fig. 3 (solid lines).

3.3. Dynamic toxicity of ZnO-NPs and $ZnCl_2$ to E. crypticus

The relationships between the survival of *E. crypticus* and the measured Zn concentrations in ZnO-NP and $ZnCl_2$ treatments at different exposure times are shown in Fig. 4. Generally, enchytraeid survival decreased with increasing Zn exposure level. At the same Zn exposure concentration, the survival decreased with time in the ZnO-NP treatments. In the $ZnCl_2$ treatments, a similar trend was only observed within 7 d of exposure, but after that survival did not further decrease with exposure time.

In the ZnO-NP series, LC50 (95% C.I.) values of Zn declined from 123 (115–131) Zn mg L^{-1} at 1 d to 67.4 (64.8–69.9) Zn mg L^{-1} at 14 d. In the $ZnCl_2$ series, the LC50 reduced from 86.4 (76.6–96.3) Zn mg L^{-1} at 1 d to 61.6 (57.9–65.4) Zn mg L^{-1} at 7 d and reached equilibrium afterwards (Table 2). The LC50 values were higher for ZnO-NPs than for $ZnCl_2$, indicating a higher toxicity of the ionic Zn. The differences in LC50s between ZnO-NPs and $ZnCl_2$ reduced with the increased exposure time, with the estimated LC50∞ values being similar at 73.5 (57.1–90.3) Zn mg L^{-1} and 63.4 (57.2–69.6) Zn mg L^{-1}, respectively. The estimated K_{e2} value was higher for $ZnCl_2$ (1.31 d^{-1}) than for ZnO-NPs (0.90 d^{-1}).

3.4. Relationship between accumulation and toxicity

The survival of *E. crypticus* exposed to ZnO-NPs and $ZnCl_2$ as a function of body Zn concentration is plotted in Fig. 5. For both ZnO-NP and $ZnCl_2$ exposures, a higher Zn level in the organisms correlated with a stronger toxic effect. When relating the survival to body Zn concentration at individual exposure times, using the logistic model (Eq. (2)), the R^2 varied from 0.18 to 0.92 for ZnO-NPs and from 0.78 to 0.99 for $ZnCl_2$ (Table 3). The better model

Table 1
Kinetic parameters (uptake rate constant K_u, bioaccumulation-based elimination rate constant K_{e1}) of ZnO-NPs and $ZnCl_2$ in *Enchytraeus crypticus* estimated by applying the one-compartment model (Eq. (1)) to the body Zn concentrations under different exposure concentration separately.

ZnO-NP treatments			$ZnCl_2$ treatments		
Zn (mg L^{-1})	K_u (mg $kg^{-1}d^{-1}$)	K_{e1} (d^{-1})	Zn (mg L^{-1})	K_u (mg $kg^{-1}d^{-1}$)	K_{e1} (d^{-1})
9.50	12.0	0.31	5.27	40.1	2.05
19.5	11.1	0.22	11.1	24.3	1.26
35.4	9.47	0.32	25.4	8.32	0.31
37.4	12.6	0.32	37.6	12.0	0.58
59.9	9.01	0.33	50.2	9.07	0.38
78.3	5.19	0.17	66.1	8.44	0.42
111	5.74	0.39			

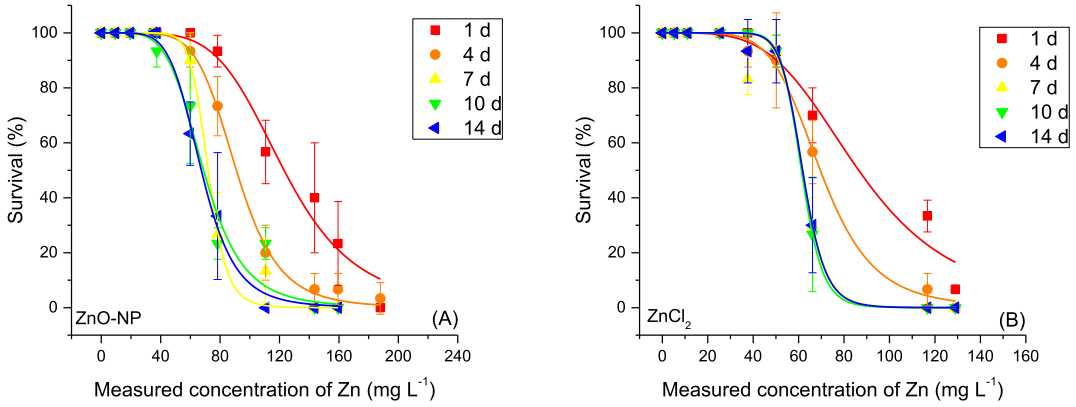

Fig. 4. Survival (%) of *Enchytraeus crypticus* after different times of exposure to different concentrations of ZnO-NPs (A) and $ZnCl_2$ (B) in test solutions embedded in a quartz sand matrix. Data points show the mean values of observed survival data with standard error for each treatment, solid lines show the fit of logistic dose-response model (Eq. (2)) to the survival data at each exposure time separately.

Table 2
LC50 values (95% confidence intervals) for the toxicity of ZnO-NPs and $ZnCl_2$ to *Enchytraeus crypticus* after different exposure times related to measured Zn concentrations in test solutions. LC50s were calculated using a logistic dose-response model (Eq. (2)). The relationship between LC50 and exposure time was described with Eq. (3), with the ultimate LC50 value ($LC50_\infty$) and toxicity-based elimination rate constant (K_{e2}) estimated.

	LC50 (mg L^{-1})					$LC50_\infty$ (mg L^{-1})	K_{e2} (d^{-1})
	1d	4d	7d	10d	14d		
ZnO-NPs	123 (115–131)	90.9 (88.9–93.1)	71.9 (68.9–75.0)	68.9 (62.2–75.5)	67.4 (64.8–69.9)	73.5 (57.1–90.3)	0.90 (±0.16)
$ZnCl_2$	86.4 (76.6–96.3)	69.5 (67.0–72.1)	61.6 (57.9–65.4)	61.3 (61.2–61.3)	61.8 (60.3–63.3)	63.4 (57.2–69.6)	1.31 (±0.15)

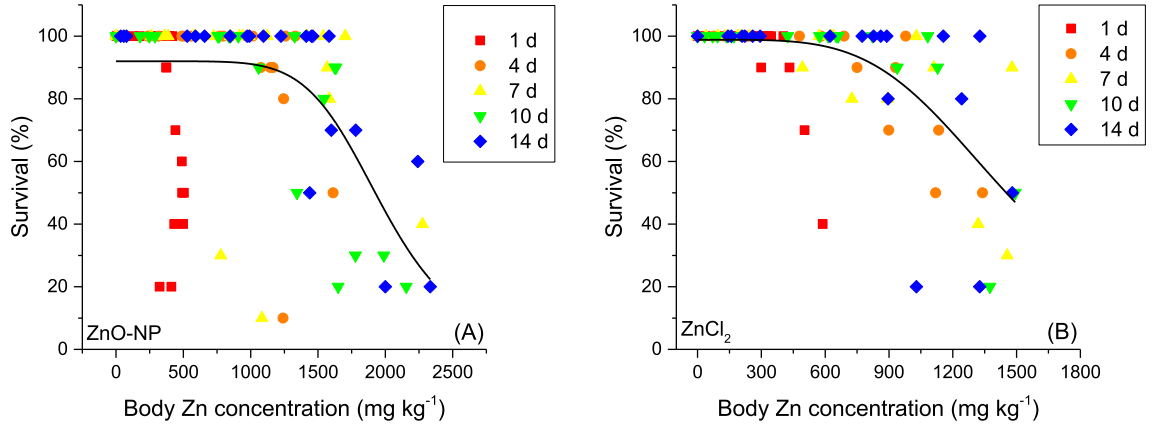

Fig. 5. Survival (%) of *Enchytraeus crypticus* exposed to ZnO-NPs (A) and $ZnCl_2$ (B) in test solutions embedded in a quartz sand matrix as a function of body Zn concentrations after different exposure times. Data points show the measured body concentration data, solid line shows the fit of a logistic dose-response curve (Eq. (2)) to all data at different exposure times together.

Table 3
LC50 values (95% confidence intervals) for the toxicity of ZnO-NPs and $ZnCl_2$ to *Enchytraeus crypticus* related to body Zn concentrations at different exposure times separately and all data together. Data were fitted to logistic dose-response model (Eq. (2)). R^2 shows the correlation between survival and body Zn concentration.

Exposure time	ZnO-NPs	R^2	$ZnCl_2$	R^2
	$LC50_{body}$ (Zn mg kg^{-1} dry body wt)		$LC50_{body}$ (Zn mg kg^{-1} dry body wt)	
1 d	461 (369–552)	0.27	448 (419–476)	0.78
4 d	1341 (291–2391)	–	1153 (1113–1193)	0.98
7 d	1590 (913–2268)	0.19	998 (812–1174)	0.98
10 d	1608 (1500–1717)	0.92	1316 (1315–1316)	0.99
14 d	1679 (634–2724)	0.18	1270 (1165–1375)	0.99
All together	1720 (1283–2156)		1306 (1179–1433)	

Table 4
Relative contribution of $NP_{(particle)}$ and $NP_{(ion)}$ to the overall toxicity and Zn bioaccumulation in *Enchytraeus crypticus* exposed to low (9.50 Zn mg L^{-1}), medium (37.4 Zn mg L^{-1}), and high (111 Zn mg L^{-1}) concentrations of ZnO-NPs after different exposure times, calculated using Eq. (4) with the concentrations of released Zn ions in the ZnO-NP suspensions as inputs.

Time	Relative contribution to accumulation (%)						Relative contribution to toxicity (%)					
	Low ZnO-NP		Medium ZnO-NP		High ZnO-NP		Low ZnO-NP		Medium ZnO-NP		High ZnO-NP	
	$NP_{(particle)}$	$NP_{(ion)}$	$NP_{(particle)}$	$NP_{(ion)}$	$NP_{(particle)}$	$NP_{(ion)}$	$NP_{(particle)}$	$NP_{(ion)}$	$NP_{(particle)}$	$NP_{(ion)}$	$NP_{(particle)}$	$NP_{(ion)}$
1 d	90.5	9.50	95.8	4.20	96.7	3.30	100	0	100	0	100	0
4 d	82.1	17.9	94.2	5.80	93.6	6.40	100	0	100	0	100	0
7 d	81.4	18.6	94.1	5.90	94.1	5.90	100	0	100	0	100	0
10 d	74.7	25.3	94.1	5.90	94.3	5.70	100	0	100	0	100	0
14 d	88.6	11.4	94.0	6.00	92.5	7.50	100	0	100	0	100	0

performance for $ZnCl_2$ than for ZnO-NP treatments demonstrates that body Zn concentration is a good indicator of toxicity for $ZnCl_2$ but not for ZnO-NPs.

From 4 to 14 d of exposure, the estimated $LC50_{body}$ (95% C.I.) values were almost constant, ranging from 1341 (291–2391) to 1679 (634–2724) Zn mg kg^{-1} dry body wt for ZnO-NPs and from 998 (812–1174) to 1270 (1165–1375) Zn mg kg^{-1} dry body wt for $ZnCl_2$ (Table 3). When fitting all data together, the estimated $LC50_{body}$ for ZnO-NPs and $ZnCl_2$ were 1720 (1283–2156) and 1306 (1179–1433) Zn mg kg^{-1} dry body wt, respectively. Although the overall $LC50_{body}$ is higher for ZnO-NPs than for $ZnCl_2$, the difference is not significant considering the overlap of the 95% confidence intervals.

3.5. Contribution of ZnO-$NP_{(particle)}$ and ZnO-$NP_{(ion)}$ to Zn accumulation and toxicity

The relative contributions of ZnO-$NP_{(particle)}$ and ZnO-$NP_{(ion)}$ to the overall accumulation and toxicity of ZnO-NPs in *E. crypticus* after different exposure times are shown in Table 4. At low ZnO-NP concentration (9.50 Zn mg L^{-1}), the contribution of ZnO-$NP_{(particle)}$ to the overall Zn accumulation varied from 75% to 91%. Accordingly, the contribution of ZnO-$NP_{(ion)}$ ranged from 9.5% to 25% during the entire exposure duration. At medium (37.4 Zn mg L^{-1}) and high (111 Zn mg L^{-1}) ZnO-NP concentrations, the contribution of ZnO-$NP_{(ion)}$ to the overall accumulation was below 7.5%. For toxicity, the relative contributions of the ions released from ZnO-NPs were negligible, approximately 0% for all treatments. This indicates that in the ZnO-NP suspensions particles rather than the released ions were the major source of toxicity.

4. Discussion

4.1. Dissolution of ZnO-NP

Our study showed that the ZnO nanoparticles underwent gradual dissolution with increasing incubation time, with fast dissolution being observed during the first 24 h. It has been shown that the percentage of ZnO-$NP_{(ion)}$ increased from 59% after 1 h of incubation to 65% after 48 h of incubation in a test medium spiked with 1–10 Zn mg L^{-1} of ZnO-NP (Xiao et al., 2015). Adam et al. (2014) reported that a large portion of dissolution occurred immediately after introducing ZnO-NPs into an aqueous test medium, with 60% dissolution within 1–2 h incubation. This is consistent with our findings. In the present study, the potential of ion release declined with increasing ZnO-NP level in suspension. Previous studies reported that the ion release percentage decreased from 58% to 44% and from 69% to 37% when ZnO-NP concentration ranged from 0.2 to 5.0 Zn mg L^{-1} and from 1.0 to 10 Zn mg L^{-1}, respectively (Bai et al., 2010; Brun et al., 2014). Exposure conditions, including exposure concentration, exposure time, and characteristics of test solutions are important factors influencing the dissolution behavior of metal-based NPs.

4.2. Accumulation and toxicity patterns of ZnO-NPs and $ZnCl_2$

Our results showed that body Zn concentration and survival of the enchytraeids in ZnO-NP and $ZnCl_2$ treatments were dependent on both exposure concentration and exposure time, with equilibrium being reached within 14 d of exposure. A similar trend of Zn bioaccumulation was found for the earthworm *Eisenia andrei* exposed to ZnO-NPs, with an initial rapid increase in internal Zn concentrations, followed by a slight decrease to equilibration within the uptake phase (Swiatek et al., 2017). For metals that could be regulated and excreted by the organism, body metal concentration would reach a stable value, while for metals that cannot be eliminated the accumulation pattern would be linear (Crommentuijn et al., 1994). The present study indicated that Zn, either ionic or in nanoparticulate form, was efficiently regulated by the enchytraeids.

For the exposure to metals in the form of metal chloride (e.g. $NiCl_2$, $CoCl_2$ and $CdCl_2$), toxic effects will occur when body metal concentration exceeds a critical level, the critical body residue (Sauvé et al., 1998), hence toxicity is closely correlated with exposure time (Broerse and van Gestel, 2010; He and van Gestel, 2013; Jager et al., 2011). The mortality of *Daphnia magna* increased with time of NiO-NP exposure (Gong et al., 2016) and the LC50 of AgNPs for *E. crypticus* decreased over time and reached steady state after 7 d (Topuz and van Gestel, 2015). These results are consistent with our finding that the toxicity of ZnO-NPs was influenced by both the exposure time and exposure concentration. Therefore, the influence of time should be considered to avoid underestimation of toxicity, especially in the case of long-term exposures to relatively low concentrations.

4.3. Toxicokinetic and toxicodynamic parameters of ZnO-NPs and $ZnCl_2$

The dynamic Zn accumulation patterns in *E. crypticus* exposed to ZnO-NPs and $ZnCl_2$ were well described by the one-compartment model. The estimated K_u and K_e values can be used to quantitively compare the differences of toxicokinetic and toxicodynamic processes of Zn in ionic and particulate form. In both ZnO-NP and $ZnCl_2$ treatments, the estimated K_u values were higher than the K_e values. It has been widely accepted that when the rate of metal uptake exceeds the rate of detoxification and elimination, the metal will accumulate in the organisms and subsequently toxic effects will be induced when the body metal concentration reaches the critical body burden (Broerse et al., 2012; Rainbow, 2007a). Moreover, metal detoxification itself is an energetically costly process, which also causes indirect physiological effects, e.g. on respiration, body size, reproduction and survival (Bednarska and Stachowicz,

2013; Sibly and Calow, 1989).

The estimated K_u values for Zn uptake from ZnO-NPs and $ZnCl_2$ tended to decline at high exposure concentrations. Consistent with the finding in the present study, Lock and Janssen (2001) found that the uptake rate constant of Cd in *Enchytraeus albidus* decreased from 0.214 to 0.104 d^{-1} when exposed to 10 and 100 Cd mg kg^{-1} dry soil. He and van Gestel (2013) and Zhang and Van Gestel (2017), investigating the toxicokinetics of Ni and Pb in *E. crypticus*, respectively, showed that uptake rate constants decreased with exposure concentration after the peak was reached. The decreased uptake rates at high exposure concentration may result from the limitation of carriers, through which metal ions could be transported through the cell membrane (Li et al., 2009). At high metal exposure concentration, cell death rate increased, and subsequently resulted in reduced toxicant absorption ability (Argasinski et al., 2012). The estimated value of K_u was higher for $ZnCl_2$ than for ZnO-NPs, indicating that ionic Zn was more accessible for *E. crypticus* than nanoparticulate Zn. Consistent with our results, the uptake rate constants were also found to be higher for ionic Zn than for nanoparticles in *E. andrei* (Swiatek et al., 2017). Diez-Ortiz et al. (2015) estimated the toxicokinetic parameters of Ag^+ ions and AgNPs for earthworms (*Lumbricus rubellus*), finding significantly higher uptake rates for the Ag^+ treatments. The aggregation of NPs in test suspensions may inhibit their uptake, as the accumulation for small ZnO-NPs was significantly than for larger ones (Kaya et al., 2016).

Compared to the uptake rate constant, the elimination rate constant is determined to a large extent by the test organism itself, and therefore is less dependent on exposure concentration (Crommentuijn et al., 1994; He and van Gestel, 2013). Overall, the bioaccumulation-based elimination rate constant (K_{e1}) and the toxicity-based elimination rate constant (K_{e2}) were above zero, meaning that *E. crypticus* was able to excrete the Zn internalized from ZnO-NP and $ZnCl_2$ exposures. Compared with ZnO-NPs, $ZnCl_2$ exposure resulted in higher elimination rates based on body concentration or survival data. Khan et al. (2015) and Topuz and van Gestel (2015), investigating the toxicokinetic and toxicodynamics of different Ag forms in *Lumbriculus variegatus* and *E. crypticus*, respectively, demonstrated that elimination rate was slower for AgNP treatments than for AgCl. However, Carbone et al. (2016) showed that the excretion rates of Ce in *Eisenia fetida* were similar when exposed to Ce ions and CeO_2-NPs, with more than 99% of Ce in the organism being excreted in five days.

The toxicokinetic and toxicodynamic patterns of Zn in ionic and particulate form were different because their uptake and elimination rates in *E. crypticus* differed from each other.

4.4. Body metal concentration versus toxicity

In the present study, at similar total Zn exposure concentrations, the body Zn concentration of *E. crypticus* was higher for ZnO-NPs than that for $ZnCl_2$, but the toxicity of ZnO-NPs was lower than that for $ZnCl_2$. It has been recognized that dissolved metals are more toxic than metal nanoparticles (Hooper et al., 2011; Lopes et al., 2014). However, despite the lower toxicity of NPs in comparison with ions, internal metal concentrations in organisms were higher for NP treatments (Heggelund et al., 2013; Topuz and van Gestel, 2015). Previously, we noticed that body metal concentration was a better predictor of toxicity as it incorporates the influence of environmental factors, including exposure conditions and exposure time (He et al., 2015; He and van Gestel, 2013). This is in accordance with the finding of the present study for $ZnCl_2$ when we linked toxicity to body Zn concentration. However, body Zn concentration was a poor predictor of the dynamic toxicity of ZnO-NPs. Bioavailability has been considered to be a dynamic process in which environmental availability of a metal causes exposure, resulting in actual uptake and subsequent effects due to the metal interacting with a biological target (Peijnenburg et al., 2007; Van Straalen et al., 2005). The metal accumulated in an organism can be metabolized and excreted, accumulated in different tissues, sequestered internally or transported to non-toxic action sites (Vijver et al., 2004). The relationship between toxicity and metal bioaccumulation may be influenced by such internal interactions, which hinder the use of body metal concentration to predict toxicity (Rainbow, 2007b). Li et al. investigated the subcellular distribution pattern of Zn in the earthworm *E. fetida*, showing that ionic Zn was distributed mainly in cell membranes and tissues, while Zn derived from NPs was stored mainly in organelles and the cytosol (Li et al., 2011). Unrine et al. (2010) and Hooper et al. (2011) showed that part of the accumulated Cu and Zn remained as particles and did not dissolve in the worm tissue. This may explain the reduced toxicity of ZnO-NPs compared to $ZnCl_2$ at similar body concentrations. Insights into the intracellular distribution and speciation of the metal are meaningful for understanding the difference in toxicity between metal-based nanoparticles and dissolved ions.

4.5. Relative contribution of ZnO-$NP_{(particle)}$ and ZnO-$NP_{(ion)}$

Currently there is no consistent information regarding the contribution of metal-based nanoparticles and their released ions to the overall toxicity and accumulation. Several studies showed that the toxicity of metal-based NPs is mainly caused by their released metal ions (Franklin et al., 2007; Heinlaan et al., 2008). For *Danio rerio* and *D. magna* the relative contribution to lethality was found to be higher for the particles than for the ions in ZnO-NP suspensions (Hua et al., 2014; Xiao et al., 2015). In the present study, we found that rather than ZnO-$NP_{(ion)}$ it was ZnO-$NP_{(particle)}$ that acted as the major source of Zn bioaccumulation and toxicity during the whole 14 d exposure period. Santo et al. (2014) and Wang et al. (2015) demonstrated that the maximum concentrations of released ions in suspensions of ZnO-NPs and Ag_2S-NPs were well below the NOEC of their ionic form for cowpea and wheat. In these cases, despite the relatively high intrinsic lethality of the metal in ionic form, the particulate metal form was the main factor causing bioaccumulation and lethality in organisms as the amount of ion released from metal-based NPs was too low to induce any significant effect.

It has been shown that ZnO-NPs and AgO-NPs can be readily taken up by earthworms (*E. fetida*) in soil (Hu et al., 2010). Similar bioaccumulation potential of Zn was found for ZnO-NPs and $ZnCl_2$ in the terrestrial isopod (*Porcellio scaber*) (Pipan-Tkalec et al., 2010). Small sized NPs can easily penetrate into embryos of zebrafish via the chorion pore canals cross the cell membrane (Lee et al., 2012). Furthermore, scanning electron microscopy analysis of earthworm tissues proved that ZnO-NPs can be taken up in particulate form by earthworms (Heinlaan et al., 2008; Hooper et al., 2011). Hence, the metals in particulate form could accumulate in organisms and subsequently cause toxicity.

5. Conclusions

In the present study, the dynamic toxicity and Zn bioaccumulation in *E. crypticus* differed greatly between ZnO-NPs and $ZnCl_2$. The estimated uptake and elimination rates of Zn were higher for $ZnCl_2$ than for ZnO-NPs, suggesting that the ionic Zn was easier to be accumulated and eliminated by *E. crypticus*. By measuring the released Zn ions in ZnO-NP suspensions, the contribution of particles and released ions to the dynamic bioaccumulation and toxicity were calculated. It was found that ZnO

particles rather than Zn ions dominated uptake and toxicity. Body Zn concentration, which integrates all steps in the toxicokinetic process, well described the dynamic toxicity of $ZnCl_2$, but not of ZnO-NPs. This may be attributed to internal distribution and detoxification mechanisms. Our study suggests that the risk assessment of ZnO-NPs cannot be conducted with the existing frameworks for conventional Zn salts. Further research on internal interactions of nanoparticles within the animals is warranted to obtain the full picture of the adverse effects of nanoparticles.

Acknowledgements

This work was supported by the National Natural Science Foundation of China (No. 41701571, No. 41701573, and No. 41877500), the National Key R&D Program of China (No. 2018YFD0800700), the 111 Project (B18060), and the Key Laboratory of Original Agro-Environmental Pollution Prevention and Control, Ministry of Agriculture/Tianjin Key Laboratory of Agro-environment and Safe-product (No. 17Z1170010019).

Appendix A. Supplementary data

Supplementary data to this article can be found online at https://doi.org/10.1016/j.envpol.2018.11.037.

References

Adam, N., Leroux, F., Knapen, D., Bals, S., Blust, R., 2015. The uptake and elimination of ZnO and CuO nanoparticles in *Daphnia magna* under chronic exposure scenarios. Water Res. 68, 249–261.

Adam, N., Schmitt, C., Galceran, J., Companys, E., Vakurov, A., Wallace, R., Knapen, D., Blust, R., 2014. The chronic toxicity of ZnO nanoparticles and ZnCl2 to *Daphnia magna* and the use of different methods to assess nanoparticle aggregation and dissolution. Nanotoxicology 8, 709–717.

Argasinski, K., Bednarska, A., Laskowski, R., 2012. The toxicokinetics cell demography model to explain metal kinetics in terrestrial invertebrates. Ecotoxicology 21, 2186–2194.

Bai, W., Zhang, Z., Tian, W., He, X., Ma, Y., Zhao, Y., Chai, Z., 2010. Toxicity of zinc oxide nanoparticles to zebrafish embryo: a physicochemical study of toxicity mechanism. J. Nanoparticle Res. 12, 1645–1654.

Bandyopadhyay, S., Plascencia-Villa, G., Mukherjee, A., Rico, C.M., José-Yacamán, M., Peralta-Videa, J.R., Gardea-Torresdey, J.L., 2015. Comparative phytotoxicity of ZnO NPs, bulk ZnO, and ionic zinc onto the alfalfa plants symbiotically associated with Sinorhizobium meliloti in soil. Sci. Total Environ. 515–516, 60–69.

Bednarska, A.J., Stachowicz, I., 2013. Costs of living in metal polluted areas: respiration rate of the ground beetle Pterostichus oblongopunctatus from two gradients of metal pollution. Ecotoxicology 22, 118–124.

Broerse, M., Oorsprong, H., van Gestel, C.M., 2012. Cadmium affects toxicokinetics of pyrene in the collembolan *Folsomia candida*. Ecotoxicology 21, 795–802.

Broerse, M., van Gestel, C.A.M., 2010. Mixture effects of nickel and chlorpyrifos on *Folsomia candida* (Collembola) explained from development of toxicity in time. Chemosphere 79, 953–957.

Brun, N.R., Lenz, M., Wehrli, B., Fent, K., 2014. Comparative effects of zinc oxide nanoparticles and dissolved zinc on zebrafish embryos and eleuthero-embryos: importance of zinc ions. Sci. Total Environ. 476–477, 657–666.

Carbone, S., Hertel-Aas, T., Joner, E.J., Oughton, D.H., 2016. Bioavailability of CeO_2 and SnO_2 nanoparticles evaluated by dietary uptake in the earthworm *Eisenia fetida* and sequential extraction of soil and feed. Chemosphere 162, 16–22.

Castro-Ferreira, M.P., Roelofs, D., van Gestel, C.A., Verweij, R.A., Soares, A.M., Amorim, M.J., 2012. *Enchytraeus crypticus* as model species in soil ecotoxicology. Chemosphere 87, 1222–1227.

Crommentuijn, T., Doodeman, C.J.A.M., Doornekamp, A., Van Der Pol, J.J.C., Van Gestel, C.A.M., Bedaux, J.J.M., 1994. Lethal body concentrations and accumulation patterns determine time-dependent toxicity of cadmium in soil arthropods. Environ. Toxicol. Chem. 13, 1781–1789.

Diez-Ortiz, M., Lahive, E., Kille, P., Powell, K., Morgan, A.J., Jurkschat, K., Van Gestel, C.A.M., Mosselmans, J.F.W., Svendsen, C., Spurgeon, D.J., 2015. Uptake routes and toxicokinetics of silver nanoparticles and silver ions in the earthworm *Lumbricus rubellus*. Environ. Toxicol. Chem. 34, 2263–2270.

Franklin, N.M., Rogers, N.J., Apte, S.C., Batley, G.E., Gadd, G.E., Casey, P.S., 2007. Comparative toxicity of nanoparticulate ZnO, bulk ZnO, and ZnCl2 to a freshwater microalga (*Pseudokirchneriella subcapitata*): the importance of particle solubility. Environ. Sci. Technol. 41, 8484–8490.

Gong, N., Shao, K., Li, G., Sun, Y., 2016. Acute and chronic toxicity of nickel oxide nanoparticles to Daphnia magna: the influence of algal enrichment. Nanoimpact 3–4, 104–109.

He, E., Baas, J., Van Gestel, C.A.M., 2015. Interaction between nickel and cobalt toxicity in Enchytraeus crypticus is due to competitive uptake. Environ. Toxicol. Chem. 34, 328–337.

He, E., van Gestel, C.A., 2013. Toxicokinetics and toxicodynamics of nickel in *Enchytraeus crypticus*. Environ. Toxicol. Chem. 32, 1835–1841.

Heggelund, L.R., Diez-Ortiz, M., Lofts, S., Lahive, E., Jurkschat, K., Wojnarowicz, J., Cedergreen, N., Spurgeon, D., Svendsen, C., 2013. Soil pH effects on the comparative toxicity of dissolved zinc, non-nano and nano ZnO to the earthworm *Eisenia fetida*. Nanotoxicology 8, 559–572.

Heinlaan, M., Ivask, A., Blinova, I., Dubourguier, H.C., Kahru, A., 2008. Toxicity of nanosized and bulk ZnO, CuO and TiO2 to bacteria *Vibrio fischeri* and crustaceans *Daphnia magna* and *Thamnocephalus platyurus*. Chemosphere 71, 1308–1316.

Hooper, H.L., Jurkschat, K., Morgan, A.J., Bailey, J., Lawlor, A.J., Spurgeon, D.J., Svendsen, C., 2011. Comparative chronic toxicity of nanoparticulate and ionic zinc to the earthworm *Eisenia veneta* in a soil matrix. Environ. Int. 37, 1111–1117.

Hu, C.W., Li, M., Cui, Y.B., Li, D.S., Chen, J., Yang, L.Y., 2010. Toxicological effects of TiO2 and ZnO nanoparticles in soil on earthworm Eisenia fetida. Soil Biol. Biochem. 42, 586–591.

Hua, J., Vijver, M.G., Richardson, M.K., Ahmad, F., Peijnenburg, W.J.G.M., 2014. Particle-specific toxic effects of differently shaped zinc oxide nanoparticles to zebrafish embryos (*Danio rerio*). Environ. Toxicol. Chem. 33, 2859–2868.

Jager, T., Albert, C., Preuss, T.G., Ashauer, R., 2011. General unified threshold model of survival - a toxicokinetic-toxicodynamic framework for ecotoxicology. Environ. Sci. Technol. 45, 2529–2540.

Kaya, H., Aydın, F., Gürkan, M., Yılmaz, S., Ates, M., Demir, V., Arslan, Z., 2016. A comparative toxicity study between small and large size zinc oxide nanoparticles in tilapia (*Oreochromis niloticus*): organ pathologies, osmoregulatory responses and immunological parameters. Chemosphere 144, 571–582.

Khan, F.R., Paul, K.B., Dybowska, A.D., Valsami-Jones, E., Lead, J.R., Stone, V., Fernandes, T.F., 2015. Accumulation dynamics and acute toxicity of silver nanoparticles to *Daphnia magna* and *Lumbriculus variegatus*: implications for metal modeling approaches. Environ. Sci. Technol. 49, 4389–4397.

Kool, P.L., Ortiz, M.D., van Gestel, C.A., 2011. Chronic toxicity of ZnO nanoparticles, non-nano ZnO and ZnCl2 to *Folsomia candida* (Collembola) in relation to bioavailability in soil. Environ. Pollut. 159, 2713–2719.

Lee, K.J., Browning, L.M., Nallathamby, P.D., Desai, T., Cherukuri, P.K., Xu, X.-H.N., 2012. In vivo quantitative study of sized-dependent transport and toxicity of single silver nanoparticles using zebrafish embryos. Chem. Res. Toxicol. 25, 1029–1046.

Li, L.-Z., Zhou, D.-M., Peijnenburg, W.J.G.M., van Gestel, C.A.M., Jin, S.-Y., Wang, Y.-J., Wang, P., 2011. Toxicity of zinc oxide nanoparticles in the earthworm, *Eisenia fetida* and subcellular fractionation of Zn. Environ. Int. 37, 1098–1104.

Li, L., Wu, H., Peijnenburg, W.J., van Gestel, C.A., 2015. Both released silver ions and particulate Ag contribute to the toxicity of AgNPs to earthworm *Eisenia fetida*. Nanotoxicology 9, 792–801.

Li, L., Zhou, D., Wang, P., Peijnenburg, W.J.G.M., 2009. Kinetics of cadmium uptake and subcellular partitioning in the earthworm *Eisenia fetida* exposed to cadmium-contaminated soil. Arch. Environ. Contam. Toxicol. 57, 718–724.

Lock, K., Janssen, C.R., 2001. Zinc and cadmium body burdens in terrestrial oligochaetes: use and significance in environmental risk assessment. Environ. Toxicol. Chem. 20, 2067–2072.

Lopes, S., Ribeiro, F., Wojnarowicz, J., Łojkowski, W., Jurkschat, K., Crossley, A., Soares, A.M.V.M., Loureiro, S., 2014. Zinc oxide nanoparticles toxicity to *Daphnia magna*: size-dependent effects and dissolution. Environ. Toxicol. Chem. 33, 190–198.

Ma, H., Williams, P.L., Diamond, S.A., 2013. Ecotoxicity of manufactured ZnO nanoparticles – a review. Environ. Pollut. 172, 76–85.

Miao, A.J., Zhang, X.Y., Luo, Z., Chen, C.S., Chin, W.C., Santschi, P.H., Quigg, A., 2010. Zinc oxide-engineered nanoparticles: dissolution and toxicity to marine phytoplankton. Environ. Toxicol. Chem. 29, 2814–2822.

Peijnenburg, W.J.G.M., Zablotskaja, M., Vijver, M.G., 2007. Monitoring metals in terrestrial environments within a bioavailability framework and a focus on soil extraction. Ecotoxicol. Environ. Saf. 67, 163–179.

Pipan-Tkalec, Ž., Drobne, D., Jemec, A., Romih, T., Zidar, P., Bele, M., 2010. Zinc bioaccumulation in a terrestrial invertebrate fed a diet treated with particulate ZnO or ZnCl2 solution. Toxicology 269, 198–203.

Qiu, H., Versieren, L., Rangel, G.G., Smolders, E., 2016. Interactions and toxicity of Cu-Zn mixtures to *Hordeum vulgare* in different soils can Be rationalized with bioavailability-based prediction models. Environ. Sci. Technol. 50, 1014–1022.

Rainbow, P.S., 2007a. Trace metal bioaccumulation: models, metabolic availability and toxicity. Environ. Int. 33, 576–582.

Rainbow, P.S., 2007b. Trace metal bioaccumulation: models, metabolic availability and toxicity. Environ. Int. 33, 576–582.

Ribeiro, F., Gallego-Urrea, J.A., Goodhead, R.M., Van Gestel, C.A.M., Moger, J., Soares, A.M.V.M., Loureiro, S., 2015. Uptake and elimination kinetics of silver nanoparticles and silver nitrate by *Raphidocelis subcapitata*: the influence of silver behaviour in solution. Nanotoxicology 9, 686–695.

Santo, N., Fascio, U., Torres, F., Guazzoni, N., Tremolada, P., Bettinetti, R., Mantecca, P., Bacchetta, R., 2014. Toxic effects and ultrastructural damages to *Daphnia magna* of two differently sized ZnO nanoparticles: does size matter? Water Res. 53, 339–350.

Sauvé, S., Dumestre, A., McBride, M., Hendershot, W., 1998. Derivation of soil quality criteria using predicted chemical speciation of Pb^{2+} and Cu^{2+}. Environ. Toxicol. Chem. 17, 1481–1489.

Schultz, C., Powell, K., Crossley, A., Jurkschat, K., Kille, P., Morgan, A.J., Read, D., Tyne, W., Lahive, E., Svendsen, C., Spurgeon, D., 2015. Analytical approaches to support current understanding of exposure, uptake and distributions of engineered nanoparticles by aquatic and terrestrial organisms. Ecotoxicology 24, 239–261.

Sibly, R.M., Calow, P., 1989. A life-cycle theory of responses to stress. Biol. J. Linn. Soc. 37, 101–116.

Swiatek, Z.M., van Gestel, C.A.M., Bednarska, A.J., 2017. Toxicokinetics of zinc-oxide nanoparticles and zinc ions in the earthworm *Eisenia andrei*. Ecotoxicol. Environ. Saf. 143, 151–158.

Topuz, E., van Gestel, C.A.M., 2015. Toxicokinetics and toxicodynamics of differently coated silver nanoparticles and silver nitrate in *Enchytraeus crypticus* upon aqueous exposure in an inert sand medium. Environ. Toxicol. Chem. 34, 2816–2823.

Tourinho, P.S., van Gestel, C.A.M., Lofts, S., Svendsen, C., Soares, A.M.V.M., Loureiro, S., 2012. Metal-based nanoparticles in soil: fate, behavior, and effects on soil invertebrates. Environ. Toxicol. Chem. 31, 1679–1692.

Tourinho, P.S., van Gestel, C.A.M., Morgan, A.J., Kille, P., Svendsen, C., Jurkschat, K., Mosselmans, J.F.W., Soares, A.M.V.M., Loureiro, S., 2016. Toxicokinetics of Ag in the terrestrial isopod *Porcellionides pruinosus* exposed to AgNPs and $AgNO_3$ via soil and food. Ecotoxicology 25, 267–278.

Unrine, J.M., Tsyusko, O.V., Hunyadi, S.E., Judy, J.D., Bertsch, P.M., 2010. Effects of particle size on chemical speciation and bioavailability of copper to earthworms (*Eisenia fetida*) exposed to copper nanoparticles. J. Environ. Qual. 39, 1942–1953.

Van Straalen, N.M., Donker, M.H., Vijver, M.G., van Gestel, C.A.M., 2005. Bioavailability of contaminants estimated from uptake rates into soil invertebrates. Environ. Pollut. 136, 409–417.

Vijver, M.G., Van Gestel, C.A.M., Lanno, R.P., Van Straalen, N.M., Peijnenburg, W.J.G.M., 2004. Internal metal sequestration and its ecotoxicological relevance: a review. Environ. Sci. Technol. 38, 4705–4712.

Waalewijn-Kool, P.L., Diez Ortiz, M., van Straalen, N.M., van Gestel, C.A.M., 2013. Sorption, dissolution and pH determine the long-term equilibration and toxicity of coated and uncoated ZnO nanoparticles in soil. Environ. Pollut. 178, 59–64.

Wang, P., Menzies, N.W., Lombi, E., Sekine, R., Blamey, F.P., Hernandez-Soriano, M.C., Cheng, M., Kappen, P., Peijnenburg, W.J., Tang, C., Kopittke, P.M., 2015. Silver sulfide nanoparticles (Ag_2S-NPs) are taken up by plants and are phytotoxic. Nanotoxicology 9, 1041–1049.

Xiao, Y., Peijnenburg, W.J.M., Chen, G., Vijver, M.G., 2016. Toxicity of copper nanoparticles to Daphnia magna under different exposure conditions. Sci. Total Environ. 563–564, 81–88.

Xiao, Y.L., Vijver, M.G., Chen, G.C., Peijnenburg, W.J.G.M., 2015. Toxicity and accumulation of Cu and ZnO nanoparticles in *Daphnia magna*. Environ. Sci. Technol. 49, 4657–4664.

Zhang, L., Van Gestel, C.A., 2017. Toxicokinetics and toxicodynamics of lead in the soil invertebrate *Enchytraeus crypticus*. Environ. Pollut. 225, 534–541.